Materials Research Bulletin 140 (2021) 111289

Contents lists available at ScienceDirect

Materials Research Bulletin

journal homepage: www.elsevier.com/locate/matresbu

Aqueous tape casting of Al_2O_3-BBSZ based LTCC multilayer substrates

Sabitha Ann Jose [a], Krishnakumar K.A. [a,b], Surendran Kuzhichalil Peethambharan [a,b,*]

[a] Materials Science & Technology Division, CSIR-National Institute for Interdisciplinary Science & Technology, Industrial Estate P.O., Thiruvananthapuram, 695019, Kerala, India
[b] Academy of Scientific and Innovative Research (AcSIR), Ghaziabad, 201002, India

ARTICLE INFO

Keywords:
Aqueous tape casting
Alumina
LTCC
Bismuth borosilicate glass
Hazard -free processing

ABSTRACT

Several volatile organic compounds (VOCs) including xylene, methyl ethyl ketone (MEK) etc. are frequently used in organic tape casting slurries. Prolonged exposure to these VOCs can lead to appalling health hazards and hence should be avoided in future for the tape casting process to be environment friendly and sustainable. In the present research, we developed an aqueous tape casting protocol for Al_2O_3-BBSZ LTCC tapes, without using VOCs. The amount of water, binder, and plasticizers were suitably optimized to yield smooth and crack-free tapes. The impressive mechanical, thermal and dielectric properties (ε_r = 7.2 and tan $\delta = 10^{-2}$ at 5 GHz) reveal that the developed aqueous protocol for tape casting is ideal for generating sustainable hybrid electronic circuits operating at extreme conditions. To the best of our knowledge, this is the first successful attempt of hazard-free aqueous tape casting of alumina-glass ceramic composite for LTCC multilayer circuit applications.

1. Introduction

In the era of hyper-scaling, the concept of hybrid multilayer circuit technology is becoming more popular, which can save space, volume, and weight, in comparison to conventional printed circuit technologies. Hybrid multilayer circuits are realized by including passive components into the substrate layers stacked horizontally and connecting them through vias, thereby providing more space to plant active components on the multilayer structure surface. The multilayer technology is broadly divided into three: (*i*) high temperature co-fired ceramics (HTCC, sintering temperature >950 °C), (*ii*) low temperature co-fired ceramics (LTCC, sintering temperature ~700–900 °C) and (*iii*) ultralow temperature co-fired ceramics (ULTCC, sintering temperature <600 °C) [1]. Compared to the HTCC process, where the electrode materials usually are low conducting molybdenum and tungsten, the main attraction of LTCC lies in its cofireability with best conductors like silver, gold, and copper. These LTCC ceramic tape substrates should possess certain characteristics for optimum applicability. They are low permittivity, low dielectric loss, temperature stability of dielectric properties, low sintering temperature (<900 °C), high thermal conductivity, matched CTE with other materials in the integration process, less toxicity, and preferably of lower cost [2].

Cofireable ceramic tapes with micron range thickness are usually realized through tape casting, a process that has the advantage of high process control to generate crack-free tapes cast onto flexible Mylar® (biaxially oriented polyethylene terephthalate) substrates [3]. The tapes are synthesized by formulating the ceramic powder into a colloidally stable slurry. In order to make the ceramic powder into a slurry, a series of additives like solvents, dispersants, plasticizers, homogenizers, and binders are used at an optimal ratio [4].

Conventional organic tape casting employs different organic solvents such as alcohols, ketones, or hydrocarbons, like xylene, ethanol, toluene, ethyl acetate, methyl ethyl ketone (MEK), etc. [5]. The principal role of the solvent is to facilitate effortless de-agglomeration and dispersion of the ceramic powder, besides maintaining inertness to the powder. Further, they should solubilize all the other organic additives. Such organic solvents ideally should possess a low boiling point, low viscosity and high vapour pressure, which helps their fast evaporation [6]. Most of the organic solvents volatilize at temperatures <100 °C, that could be inhaled by the user besides being inflammable. Despite immense merits, the main disadvantage of organic tape casting is their high level of toxicity on prolonged exposure. For example, xylene, the central component in most organic tape casting, whose vapours when inhaled as small as 100 ppm, can affect the nervous system and cause nausea, but may even lead to death when exposed to >10,000 ppm [7,8]. Further, continuous exposure of mixed organic solvents like xylene, benzene, and toluene can even influence menstrual cycles in women and are inimical to the healthy reproductive process in men [7]. A recent study suggests

* Corresponding author.
E-mail address: kpsurendran@niist.res.in (S. Kuzhichalil Peethambharan).

https://doi.org/10.1016/j.materresbull.2021.111289
Received 28 July 2020; Received in revised form 18 December 2020; Accepted 28 February 2021
Available online 4 March 2021

that prolonged breathing of many of the volatile organic compounds (VOCs), including MEK, can lead to respiratory diseases, anaphylactic diseases, cardiovascular diseases, and even cancer [9,10]. On top of this, the CO_2 emission and climate impact in many of the solvent-based processes is also alarmingly high, since VOCs can alter the nitrogen deposition rates and mean annual temperatures [11]. That means, despite the advantages like ambient evaporative drying and avoidance of hydration of the ceramic powder, the solvent-based process demands special precaution on managing the toxicity. In a recent study, it was shown that the overall rise of CO_2 in the atmosphere could be reduced to 29 % from 43 % if the organics are replaced by aqueous components [12]. In the aqueous process, no organic solvent recovery systems are required to control the emission of volatile compounds into the atmosphere. Earlier reports suggest that aqueous slurry has inferior tolerance to changes in drying conditions and less control over film thickness [13]. Hence the selection of the slurry components should be highly critical to ensure high solid loading, uniform and defect-free thermal shrinkage during post cast drying, microstructural homogeneity, ability to stand high thermo-compression, and high mechanical strength after firing.

Besides water-miscible solvents, finding a proper binder is another hurdle, since it should be soluble in water and also provide enough strength among filler particles through organic bridges, after evaporating water. A wide range of water-soluble binders like cellulose ethers, polyvinyl alcohol, acrylic polymer, acrylic polymer emulsion, etc. have been studied for tape casting [14]. Nevertheless, this procedure has to keep up with stringent conditions to obtain a tape without detrimental defects [15]. Some of the drawbacks concerning the aqueous tape casting are namely, (*i*) slow rate of evaporation of the solvent, (*ii*) high binder concentration required for good cohesion, (*iii*) hydrogen bonding results in agglomeration which eventually leads to flocculation of the slurry and (*iv*) reaction with hygroscopic ceramic powders [15]. It is very important to study aqueous LTCC tapes based on alumina due to their superior properties like small dielectric constant, less loss, low cost, etc. Generating crack-free homogeneous LTCC tapes following aqueous slurry method is a great challenge, which is candidly taken up in the present research. In order to overcome some of the inherent shortcomings of water-based slurries in post cast drying, critical care has been given to formulate suitable aqueous slurries that can generate high-density alumina tapes and substrates.

Recently, Nina et al. reported the environment friendly tape casting of two ULTCC materials, copper molybdate and copper molybdate-Ag_2O, for multilayer substrates using tape casting [16]. Though ULTCC research is still in the early stage of development, these results supplement the present aqueous approach of developing sustainable LTCC technology. Traditionally, bismuth zinc borosilicate (BBSZ) glass with composition 35 Bi_2O_3:32 ZnO:27 B_2O_3:6 SiO_2, has been used in LTCC research as a vitreous sintering agent [17]. There are earlier reports on BBSZ glass successfully employed in reducing the sintering temperature of high-temperature ceramics [18,19]. In 2015, Induja et al. proved that Al_2O_3-BBSZ is an ideal system for developing high thermal conductivity ceramic tapes by following a non-aqueous solvent route [20]. In 2017, Chen et al. suggested Al_2O_3–BBSZ composite as a suitable material for ULTCC application where sintering was made possible at a temperature as low as 450 °C [21]. None of these studies explores the tape casting of any alumina-glass ceramic composite using aqueous slurries, which is technologically important due to the abundance of alumina and also since water can support long-range inter-particle electrostatic forces, which can eventually improve slurry dispersion and solid loading.

Thus, this work aims to devise a sustainable approach by eliminating harmful organic additives in tape casting slurry, thereby enabling a lower carbon footprint. A successful protocol to synthesize LTCC aqueous tapes was formulated with the help of suitable binders and dispersants. In the present work, we incorporated a systematic development of the aqueous route of LTCC, 40 wt. % Al_2O_3- 60 wt. % BBSZ tapes and studied how aqueous route had changed the properties of tapes from the previously reported conventional route [20].

2. Experimental section

2.1. Preparation of BBSZ glass and Al_2O_3-BBSZ composite

Already reported quenching method was used to prepare Bismuth zinc borosilicate glass (35 Bi_2O_3:32 ZnO:27 B_2O_3:6 SiO_2, BBSZ) [20]. High purity Bi_2O_3 (99.9 %, Sigma Aldrich), ZnO (99.9 %, Sigma Aldrich), B_2O_3 (99 %, Sigma Aldrich), and SiO_2 (99.6 %, Sigma Aldrich) were used. The amorphous nature of the BBSZ glass was confirmed by XRD (CuKα radiation, PANalytical X'Pert Pro diffractometer). The alumina powder (Al_2O_3, Nippon Light Metal Co. Ltd., Japan) and 60 wt. % glass was ball milled together using distilled water medium for 24 h to get a homogeneous mixture

2.2. Preparation of Al_2O_3 –BBSZ tapes

In the present study, instead of conventional two-step slurry preparation, we followed a single-stage preparation by adding all the slurry forming chemicals in one stage. Herein, a homogeneous mixture of 60 wt.% of BBSZ glass with 40 wt.% of alumina powder was used. The water-soluble binder WB4101, plasticizer PL002 compatible with the binder system, and a non- silicon defoamer DF002 (Haiku Tech B.V., The Netherlands) along with distilled water were used as the vehicle components of the tape casting slurry. The commercial binder WB4101 essentially consists of an aqueous solution of an acrylic polymer copolymerized with several dielectric loving functional groups. Here, the binder used has low toxicity levels and offers low environmental hazard. Also, the binder acts as a dispersant as well and can offer high strength and packing density in ceramic laminates. The optimal colloidal stability of the system is important to obtain a uniform and homogeneous tape. The slurry with an adequate volume of filler, binder, plasticizer, and defoamer were dispersed in distilled water which acts as solvent and was ball milled for 48 h. In the present study, the ceramic powder was made into an aqueous colloidal solution where WB4101 acts as a binder and dispersant. The concentration of WB4101 to solid loading was varied from 33 %–40 %. We kept the plasticizer (PL002) to defoamer (DF002) ratio fixed at 1:1. The viscosity of the slurry for different concentrations of the binder with respect to the filler was measured using a rheometer (Rheoplus32, Anton Paar, USA). The optimally flowing slurry was cast as thin ceramic tapes with appropriate thickness using a tape casting machine (Keko equipment, Zuzemberk, Slovenia) onto a Mylar® film whose one side is coated with silicon. The cast tapes were allowed to dry for 48 h in dry air. The dried green tape was laminated using the isostatic laminating press (Keko equipment, Haikutech, Maastricht, Netherlands) at a temperature of 70 °C under a pressure of 5 MPa for 15 min. To avoid warping, these tapes were subjected to constrained sintering at 900 °C.

2.3. Characterization

The thermal decomposition of the tapes was measured using the thermogravimetric analyzer, TGA (Perkin Elmer, Waltham, USA) the measurement was taken in air up to 1000 °C using a green tape sample. The thermal properties of the alumina-glass LTCC tapes were studied by pressing them into thick substrates of suitable dimensions and sintering at 900 °C, followed by machining. The coefficient of thermal expansion (CTE) of Al_2O_3-BBSZ tapes was measured by thermomechanical analyzer (TMA SS7300, SII Nano Technology Inc, Northridge, CA, USA). The linear expansion coefficient (α_l) was calculated for the temperature range $T_1 < T < T_2$ using the equation,

$$\alpha_l = \frac{L_2 - L_1}{L_1(T_2 - T_1)} \quad (1)$$

where L_1 and L_2 are the length of the specimen at temperature T_1 and T_2, respectively. The thermal conductivity of the sintered tape was measured using a xenon flash thermal properties analyzer

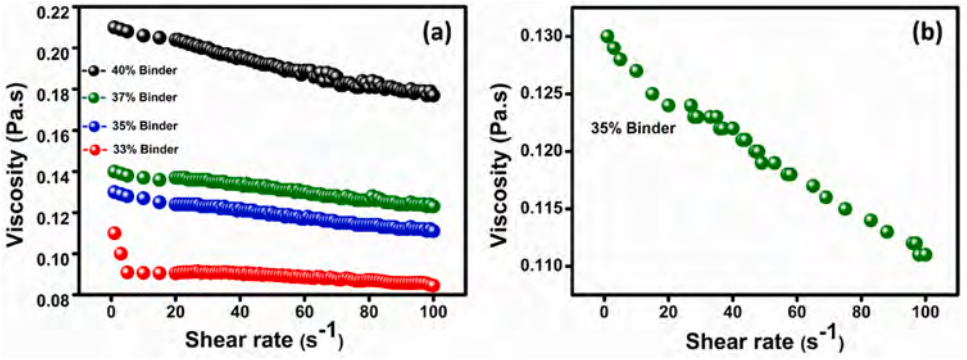

Fig. 1. (a) Variation of viscosity with different wt.% of binder and (b) viscosity of the optimized alumina-BBSZ tape casting slurry.

(FlashLine2000, Anter Corporation, Pittsburgh, USA). The specifically machined ceramic sample was subjected to a short burst of energy using an IR flash gun. With the assumption that the energy absorbed by the sample and the reference sample is similar, the specific heat can be calculated using the following equation

$$C_{sample} = \frac{(mC\Delta T)_{ref}}{(m\Delta T)_{sample}} \quad (2)$$

The resulting temperature rise on the rear side of the sample was measured as a function of time with the help of a detector. The time taken by the material to reach 50 % of the maximum temperature (t_{50}) and the thickness of sample (a) were used to calculate the diffusivity (D) using Parker relation [22].

$$D = \frac{0.139a^2}{t_{50}} \quad (3)$$

The thermal conductivity (K) can be calculated from the measured value of D, and C_{Sample}, along with the known density (ρ) of the specimen by the following equation,

$$K = DC\rho \quad (4)$$

Using a universal testing machine (Hounsfield, H5K-S UTM, Redhill, UK), the mechanical strength of the tape was measured. The micro-hardness of the sintered tapes was measured using Vicker's micro indentation hardness test (Shimadzu HMV-2TAW, Kyoto, Japan). The test is generally conducted with a square base diamond pyramid as the indenter. The applied load by the surface area of the indentation gives the Vickers hardness number (VHN),

$$VHN = \frac{2P\sin\frac{\theta}{2}}{L^2} \quad (5)$$

where P is the applied load, θ is the angle between the opposite faces of the indenter, and L is the average length of the diagonal obtained from the indentation. SEM (JOEL-JSM 5600 L V, Tokyo, Japan) was used to study the microstructure of the sintered and green tapes while the surface roughness was measured using atomic force microscopy, AFM (Bruker, Nano, USA) in tapping mode. Split post dielectric resonator (QWED, Warsaw, Poland) operating at frequencies 5 GHz with the aid of a Vector Network Analyzer (E5071C, Agilent Technologies, Santa Clara, CA) was used to measure microwave dielectric properties of the sintered tape.

3. Results and discussion

Aqueous LTCC technology is less explored; this research is important in terms of its environmental friendliness. The initial step in tape casting is the optimization of the viscosity of the slurry to obtain uniform and homogeneous tapes. As stated earlier, the slurry formation was carried out in single stage and, WB4101 is used to obtain higher powder loading.

Table 1
Composition of Al_2O_3-BBSZ aqueous LTCC tape.

Material	Function	Quantity (wt. %)
Al_2O_3- BBSZ composite	Filler	47.0
Water	Solvent	31.3
WB4101	Dispersant/Binder	18.8
PL002	Plasticizer	1.4
DF002	Defoamer	1.4

Fig. 1(a) depicts the variation of viscosity of the developed slurries with different binder concentrations (33 %–40 %).

It is evident from the graph that as the amount of binder increases, the viscosity is increasing. We could observe a sharp increase of viscosity from 37 % to 40 % of binder with respect to the filler. This means we have exceeded the optimal binder levels, which increases free polymers in the slurry and generates bridging flocculation, causing the suspension viscosity to suddenly elevate [23]. Hence higher viscosity values were avoided for the tape casting process. Since WB4101 has dual roles to play, like stabilizing the slurry and binding the particles together, an optimum value of it is required among the other weight percentages to maintain good tape quality after drying [24]. Cracks were observed for lower binder concentration (33 %). After casting and assessing the green tape quality, binder concentration was optimized to 35 %. Fig. 1(b) gives a clear picture of the variation of viscosity with shear rate for the optimized concentration of binder. The viscosity decreases with an increase in shear rate, the shear-thinning behaviour essential for the tape casting slurry is evident here. The breaking of weak intermolecular bonds and the presence of liquid layer in-between the solid ceramic particles are the reasons in reducing viscosity [25,26]. The synthesized slurry is well dispersed and homogeneous, whose composition is given in Table 1. High amounts of plasticizers are required in aqueous tape casting as compared to the conventional tape casting since most of the water-soluble binders are sensitive to moisture after drying [27]. In the present study after inspecting the green tape quality, the weight percentage of plasticizer and defoamer were maintained at 1:1 with respect to the powder loading.

In order to study the thermal decomposition of the organic additives employed in tape casting, the thermogravimetric (TG) analysis of the green tape was carried out. It is crucial to remove the organic additives prior to sintering to avoid unnecessary effects of them on the material properties [3]. The TG measurement was taken in air atmosphere up to 1000 °C, and the corresponding thermogram is shown in Fig. 2(a). The thermal degradation of the tape was obtained, with a flat curve after 500 °C. With the increase in temperature from room temperature, a sharp weight loss of about ~9 % was obtained in the temperature range from 100 °C to 320 °C [20,3]. The thermogravimetric weight loss within this interval is due to the evaporation of water and low molecular weight additives. Further, a weight loss of about 10 % observed between 320 °C–480 °C, mainly attributed to the binder burnout beyond which there

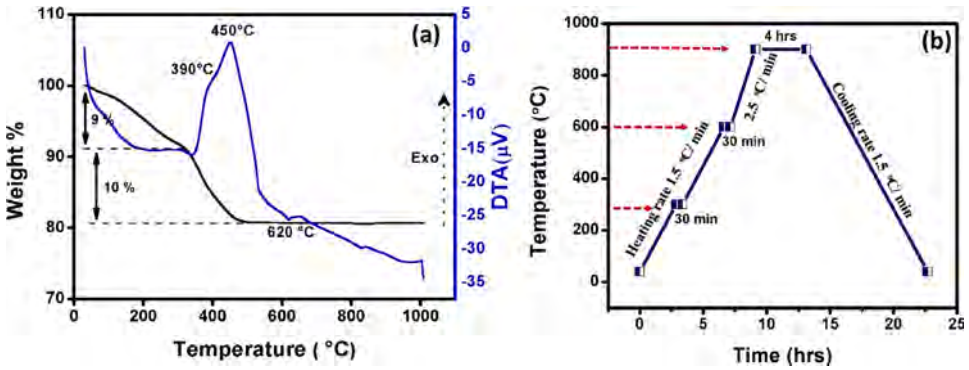

Fig. 2. (a) TG/DTA plot of the LTCC green tape, (b) sintering profile of LTCC tape.

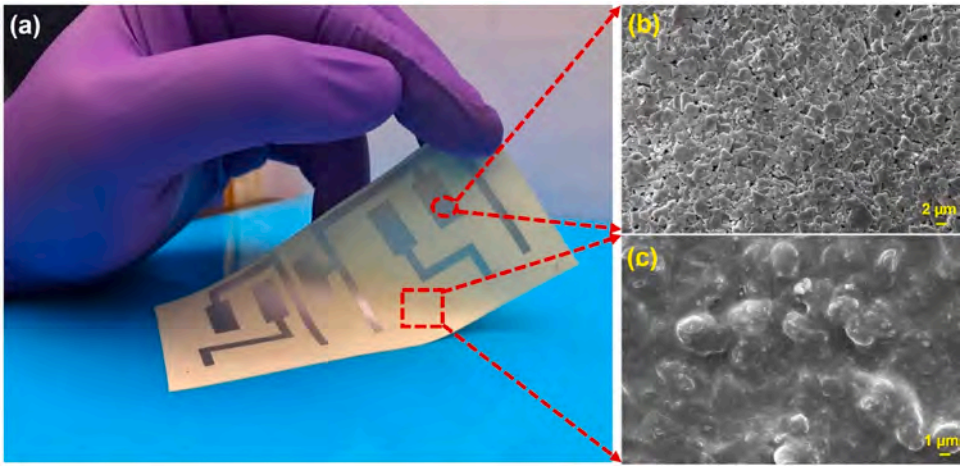

Fig. 3. (a) Photograph of silver ink screen printed on the green tape, (b) SEM image of the printed silver ink and (c) SEM image of the surface of green tape.

is no further gravimetric weight loss observed [28]. The exothermic peaks at around 390 °C and 450 °C in DTA is due to the release of heat energy due to the burning of organic additives in the tape. The endothermic peak at 620 °C corresponds to the energy absorbed during the melting of the BBSZ glass. The DTA of prepared BBSZ glass is given in Fig. S1 [29]. The minor exothermic peak around 800 °C could be attributed to the phase transition of alumina [30–32]. Based on a systematic analysis of additive decomposition from TG, we designed a sintering profile for aqueous Al_2O_3-BBSZ tape, as shown in Fig. 2(b). The tape was sintered at 900 °C with two intermediate dwells at 300 °C and 600 °C, aiming complete burn out of the binders.

The properties of green tapes, like flexibility, tensile strength, etc. play a greater role in LTCC substrate applications. In fact, the prepared green tapes will undergo many processes prior to cofiring. Printing of conductive inks on the surface is of utmost importance [33]. Fig. 3(a) shows the photograph of a flexible green tape screen printed with homemade silver ink. Fig. 3(b) shows the SEM image of the surface of Al_2O_3-BBSZ green tape screen-printed with Ag paste, and we could observe a plate-like microstructure, where the majority showing triangular morphology with some porosity as could be inferred from the black portions in the micrograph. Fig. 3(c) represents the micrograph of the obtained green tape. As discussed earlier, the amount of binder used in aqueous tape casting is more compared to the conventional non-aqueous route; this could be clearly visible from the image. It is observed that the ceramic filler particles are encapsulated with a thick binder layer, which makes it difficult to distinguish between the

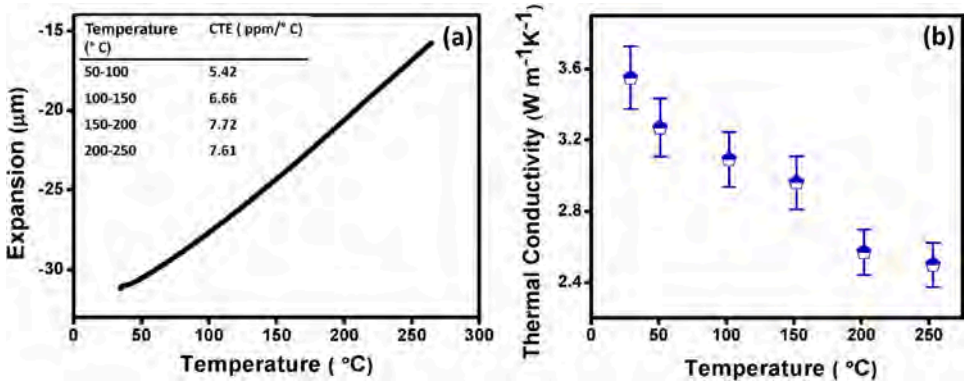

Fig. 4. (a) Thermal expansion characteristics and (b) variation of thermal conductivity of the aqueous derived LTCC tape, as a function of temperature.

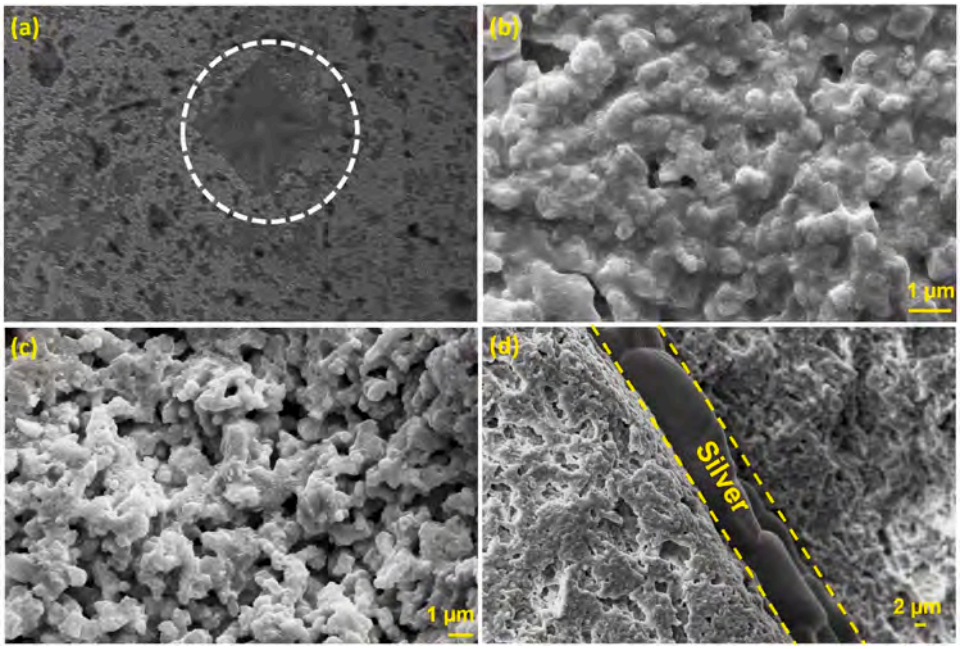

Fig. 5. (a) Indentation produced by Vicker's indenter on the surface of Al_2O_3-BBSZ tape (Optical microscope image). (b), (c) and (d) SEM images, surface of sintered tape, cross section of sintered tape and stacked sintered tape incorporated with Ag.

particles.

Fig. S2 shows the XRD pattern of the sintered tape at 900 °C. Apart from the peaks of Al_2O_3 (JCPDS file card no:01-075-1862), additional secondary phases were also formed. Along with the already reported thermodynamically stable $ZnAl_2O_4$ (JCPDS file card no: 00-005-0669), phases of $Bi_{24}Si_2O_{40}$ (JCPDS file card no:01-080-0627) and Bi_2O_3 (JCPDS file card no:01-074-1373) could also be identified as the secondary phase from the XRD [21,20]. In most of the glass-ceramic systems, including commercially available LTCC compositions, the glass phase reacts with the filler to form additional secondary phases. This secondary phase has the potential to alter the properties of the glass-ceramic system dramatically [20]. Many factors like the sintering temperature, properties of prepared glass which in fact depends on the heating and cooling rate of the glass formation, etc., crucially determines secondary phase formation [34,35]. XRD confirming the formation of BBSZ glass is given in Fig. S3.

In LTCC substrate application, thermal properties play a major role since the substrate undergoes several stresses due to different thermal expansivity of the tapes and electrodes. During cofiring, a mismatch in the thermal expansion coefficient can create cracks and delamination [36,37,3]. From Fig. 4(a), the CTE value of Al_2O_3-BBSZ is found to be 6.8 ppm/°C which falls within the acceptable limit as ceramic materials generally have low CTE values ranging from 0.5 to 15 ppm/ °C. In 2017, Roshni et al. reported zinc aluminate-titanate composite (ZAT) to have a CTE value of 6.59 ppm/°C [38]. Only a few reports are available with high CTE values. In 2018, Xiang et al. studied $CaMgGeO_4$ microwave

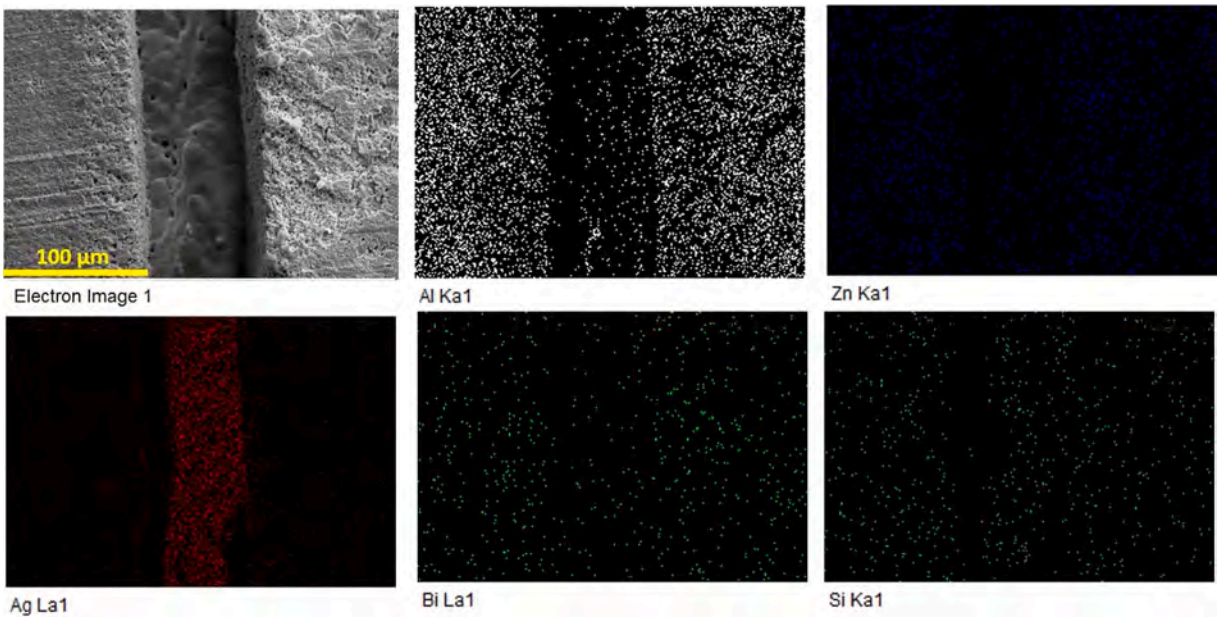

Fig. 6. SEM- elemental maps of the cross- section of the sintered tape incorporated with Ag.

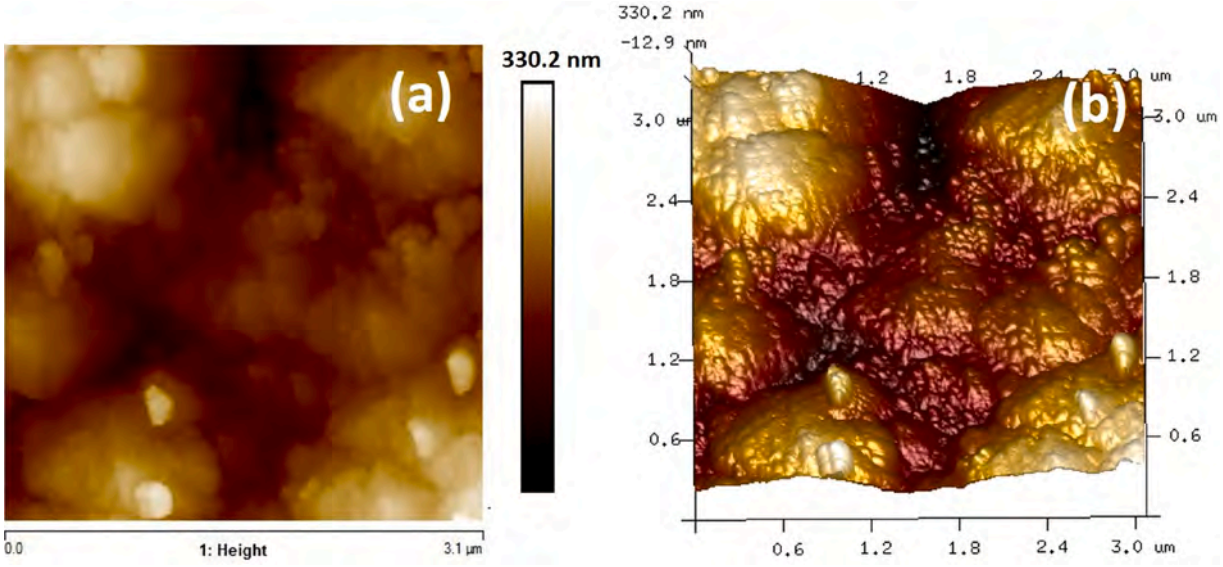

Fig. 7. (a) 2D AFM image and (b) 3D AFM image of Al_2O_3-BBSZ sintered tape.

dielectric ceramics, which has a CTE value of 12.4 ppm/°C [36]. The present CTE value obtained is well in range with the alumina substrates. Besides thermal expansion, thermal conductivity is also critical in multilayered ceramics. Usually, the thermal conductivity of LTCC substrate is ten times higher than that of organic laminates [39]. However, the thermal conductivity of LTCC tape is much less compared to high temperature cofired ceramics (HTCC) due to the presence of glass as the sintering aid in most LTCC tapes. The variation of thermal conductivity of Al_2O_3- BBSZ as a function of temperature is shown in Fig. 4(b). At room temperature, the thermal conductivity is found to be 3.55 Wm^{-1} K^{-1}. Thermal conductivity also depends highly on the microstructure of the material. In alumina based glass-ceramic composites, due to the poor thermal properties of the glass or the entrapped porosity of the composite, thermal conductivity values generally fall in the range 2−3 Wm^{-1} K^{-1} [28].

Even though glass addition successfully lowered the sintering temperature, but at the stake of sacrificing the mechanical properties of the ceramic substrate [40]. Even the slightest amount of glass will greatly deteriorate the hardness of the ceramic, which limits the machinability for cutting, via punching, etc., on the substrate [41,4]. The microhardness measurement using the Vickers hardness test is a versatile tool to measure the mechanical strength of the sintered body [42]. The average value of Vickers hardness number after five measurements was found to be 73.48 with a standard deviation of 6.72. The hardness of the Al_2O_3-BBSZ tape is found to be 0.72 GPa. This value is in good agreement with the previous reports [43,44]. The tensile strength of the green tape was measured using the sample with a thickness of 112 µm. It was found that a single layer of the unsintered sample had a tensile strength of 0.43 MPa, which is falls in the range of previous reports [45].

Indentation produced by Vicker's indenter is depicted with the help of optical micrographic image of the surface of Al_2O_3-BBSZ tape in Fig. 5 (a). The SEM image of the surface and cross-section of the sintered tape is shown in Fig. 5(b) and (c), respectively. The close inspection of the micrographs clearly shows the glassy phase in melted form. Since in our tapes, we used high amount of glass compared to ceramic filler, more melted glass is evidently seen in the micrograph. The diffusion of silver into the substrate material and its partial evaporation from the material surface are the two important challenges that should be addressed during co-firing ceramic with Ag in LTCC technology. To test the diffusion of Ag into the LTCC tape matrix, Ag was blanket printed on the green tape and was thermo laminated together and sintered. Ag paste after sintering at 900 °C for 4 h transforms to a well-densified microstructure. The cross-sectional microstructure of the cofired LTCC tape given Fig. 5(d) testifies less diffusion into the interior of the tape. The SEM image of the surface of the blanket printed silver on top of the tape sintered (at 900 °C) is given in Fig. S4. Evidently, these grains show symptoms of partial melt crystallization. The triangular morphology of the freshly printed silver on LTCC tapes as depicted in Fig. 3(b) was converted to a dense polyhedral microstructure.

Table 2
Microwave dielectric properties of aqueous LTCC tapes at 5 GHz.

Material	No. of layers	Thickness (mm)	Permittivity (ε_r)	Dielectric loss tangent (tan δ)
Green Tape	1	0.15	4.93	0.08
Sintered stack	5	0.72	7.2	0.01

To further confirm the extend of silver diffusion into the substrate, elemental mapping at the microstructure level was carried out. Fig. 6 shows the elemental mapping of the cross-section of the cofired Al_2O_3-BBSZ tape. From this, it is clear that the diffusion of silver into the substrate is very minimal. We observed a very less percentage of silver in the substrate region, which could be caused due to many factors like (i) during the printing and lamination process, (ii) during the sample preparation for SEM, and (iii) use of silver nanoparticle ink, etc. The melting point of Ag ink is less compared to the actual melting point of bulk silver, eventually contributing to some minute level of diffusion [46]. Apart from this, most of the printed silver concentration is found in between the two layers of sintered tapes.

After sintering, smooth surfaces of the tapes are preferred since it is beneficial for soldering of the conductors onto the substrate and reduce circuit loss [36]. Fig. 7(a) and (b) show the 3D and 2D AFM images of sintered tapes, respectively. The average surface roughness of the polished sintered tape is found to be 123 nm with an RMS value of 189 nm. This means, the post sintering microstructure of aqueous derived tapes are much similar to organically derived tapes. Most of the commercial tapes show a surface roughness <500 nm/ square inch, and the developed green and sintered tape's roughness are in good agreement with the commercial values.

Table 2 gives the microwave dielectric properties of the single-layer green tape and stacked sintered tapes at a specific frequency of 5 GHz, measured using SPDR. The green tape has a lower value of relative permittivity compared to sintered tapes. This is mainly because of the

Table 3
Comparison of properties of BBSZ/Al_2O_3 composite tapes with literature and commercial LTCC materials.

Sl. No.	Material	ε_r	Loss	TEC	Reference
Reported compositions					
1	KABS & ZBS glass/alumina (70 wt% :30 wt%)	4.92	0.002 @ 14 GHz	5.5	[47]
2	KBSA glass/alumina (60 wt %:40 wt %)	5.60	0.0019 @ 1 MHz	9.4	[48]
3	CBS glass/alumina (50 wt %:50 wt%)	8.06	0.0012 @ 7 GHz	5.47	[49]
4	Ca–Al–B–Si–O glass/alumina (65 wt%:45 wt%)	7.82	0.00053 @ 10 MHz	–	[50]
5	Commercial DL828 AGC glass powder/alumina (70 wt%:30 wt%)	4.08	0.007 @ 1 MHz	4.38	[51]
6	CABS/ alumina (55 wt %:45 wt%)	7.92	0.001 @ 7 GHz	5.6	[52]
7	LABS glass/alumina (60 wt %: 40 wt %)	4.70	0.005 @ 5 GHz	5.1	[28]
8	BBSZ glass/alumina (60 wt %: 40 wt %) [non-aqueous]	10.9	0.009 @ 5 GHz	–	[20]
9	BBSZ glass/alumina (60 wt %: 40 wt %) [aqueous]	7.20	0.01@ 5 GHz	6.8	Current work
Commercial LTCC materials					
10	Ferro A6M	5.90	0.002 @ 10 MHz	5.8	[53]
11	Dupont 951	7.80	0.0015 @ 1KHz	7	[54]
12	Heraeus CT700	7.00	0.002 @ 1KHz	6.7	[55]

presence of pores and organic additives like binders, plasticizers and homogenizers. Most of the organic materials have high dielectric loss with low dielectric constant because of strong covalent bonding and lower atomic polarizability [28]. In the sintering process, burnout of organics results in reduction of porosity and the material undergoes densification to a rigid ceramic. This obviously will improve the relative permittivity and reduce the dielectric loss. At 5 GHz, the sintered BBSZ-Al_2O_3 tapes of 0.72 mm thickness shows a dielectric constant, $\varepsilon_r = 7.2$ and dielectric loss, tan $\delta = 0.01$. Compared to the previously reported conventional Al_2O_3-BBSZ LTCC tapes, the obtained dielectric constant is lesser, which is beneficial in electronic packaging as it will reduce the signal propagation delay, while the dielectric loss is almost comparable [1]. This difference in the dielectric constant is mainly due to the difference in the secondary phase formation during both processes [20].

Finally, the performance of presently developed aqueous Al_2O_3/BBSZ tapes are compared with properties of different Al_2O_3/glass composites and commercial LTCC materials, as given in Table 3. From the Table, it is evident that the present aqueous derived LTCC tapes show comparable values with previous reports and commercial tapes, which qualifies aqueous tape casting a promising sustainable alternative to the conventional organic tape casting process.

4. Conclusions

In an age when climate change has become an imminent reality, the usage of volatile organic compounds (VOCs) in conventional tape casting should be avoided. This is because the commonly used solvent in the organic slurry making, xylene can result in acute health hazards when inhaled for prolonged durations. Inspired by these needs, we herein developed a sustainable water-based tape casting method, useful for LTCC tape substrates. A systematic study of the properties of 60 % BBSZ–40 % alumina composition for LTCC was carried out. From trial and error and from the rheological studies, the amount of binder was optimized to 35 wt. % for LTCC. In order to reduce the sintering temperature of HTCC alumina, 60 wt. % of BBSZ glass was added, resulting in the sintering of the glass-ceramic to happen at 900 °C. The tensile strength of alumina-BBSZ green tapes was found to be 0.42 MPa, while their mechanical hardness after sintering was estimated as 0.72 GPa. The thermal expansion coefficient and thermal conductivity of the LTCC tapes were measured to be 6.8 ppm/°C and 3.55 Wm^{-1} K^{-1}, respectively. The microwave dielectric properties and thermal stability of dielectric properties reveal that the aqueous protocol adopted in the present research to develop flexible ceramic tape can be ideal to LTCC tapes that find immense applications in hybrid electronic circuits operating at extreme conditions. The present research defies the conventional belief that aqueous slurry has inferior tolerance in various drying conditions due to slower solvent evaporation rates and less control over film thickness. By meticulously choosing and controlling the vehicle components, aqueous tape casting can yield uniform LTCC tapes, besides enabling the processing at lower health hazard levels.

CRediT authorship contribution statement

Sabitha Ann Jose: Data curation, Writing - original draft. **Krishnakumar K.A.:** Conceptualization. **Surendran Kuzhichalil Peethambharan:** Supervision, Resources, Conceptualization, Validation.

Declaration of Competing Interest

The authors declare that they have no known competing financial interests or personal relationships that could have appeared to influence the work reported in this paper.

Acknowledgements

The authors acknowledge the Technology System Development Project (DST/TSG/2015/359) funded by the Department of Science and Technology, New Delhi. The authors appreciate the help from Mr. Kiran Mohan and Mr. V. Harish Raj, respectively, for TEM and SEM analysis. The authors are also thankful to Dr. U. S. Hareesh, Mr. Peer Mohammed, and Mr. Firoz for the rheology measurements.

Appendix A. Supplementary data

Supplementary material related to this article can be found, in the online version, at doi:https://doi.org/10.1016/j.materresbull.2021.111289.

References

[1] M.T. Sebastian, Dielectric Materials for Wireless Communication, Elsevier Science, 2010.
[2] M.T. Sebastian, H. Jantunen, Microwave materials and applications, 2 Volume Set | Wiley, in: M.T. Sebastian, R. Ubic, H. Jantunen (Eds.), Microw. Mater. Appl., Wiley, 2017, pp. 355–408.
[3] P. Abhilash, M.T. Sebastian, K.P. Surendran, Glass free, non-aqueous LTCC tapes of Bi4(SiO4)3 with high solid loading, J. Eur. Ceram. Soc. 35 (2015) 2313–2320.
[4] S. Arun, M.T. Sebastian, K.P. Surendran, Li_2ZnTi_3O8 based High κ LTCC tapes for improved thermal management in hybrid circuit applications, Ceram. Int. 43 (2017) 5509–5516.
[5] L. Ren, X. Luo, H. Zhou, The tape casting process for manufacturing low-temperature co-fired ceramic green sheets: a review, J. Am. Ceram. Soc. 101 (2018) 3874–3889.
[6] R. Greenwood, E. Roncari, C. Galassi, Preparation of concentrated aqueous alumina suspensions for tape casting, J. Eur. Ceram. Soc. 17 (1997) 1393–1401.
[7] R. Kandyala, S.P. Raghavendra, S. Rajasekharan, Xylene: an overview of its health hazards and preventive measures, J. Oral Maxillofac. Pathol. 14 (2010) 1.
[8] K. Niaz, H. Bahadar, F. Maqbool, M. Abdollahi, A review of environmental and occupational exposure to xylene and its health concerns, EXCLI J. 14 (2015) 1167–1186.
[9] J. Shuai, S. Kim, H. Ryu, J. Park, C.K. Lee, G.B. Kim, V.U. Ultra, W. Yang, Health risk assessment of volatile organic compounds exposure near Daegu dyeing industrial complex in South Korea, BMC Public Health 18 (2018) 1–13.
[10] W. Miekisch, J.K. Schubert, G.F.E. Noeldge-Schomburg, Diagnostic potential of breath analysis - focus on volatile organic compounds, Clin. Chim. Acta 347 (2004) 25–39.

[11] J.V.H. Constable, M.E. Litvak, J.P. Greenberg, R.K. Monson, Monoterpene Emission From Coniferous Trees in Response to Elevated CO_2 Concentration and Climate Warming, Wiley-Blackwell, 1999, https://doi.org/10.1046/j.1365-2486.1999.00212.

[12] J. Stiernstedt, Environmental and Quality Analysis of Aqueous Tape Casting Chalmers Area of Advance on Sustainable Production View Project Prospective Battery LCA View Project, 2011.

[13] J. Huang, Y. Jinlong, Novel Colloidal Forming of Ceramics, Springer, 2011.

[14] D. Hotza, P. Greil, Review: aqueous tape casting of ceramic powders, Mater. Sci. Eng. A 202 (1995) 206–217.

[15] A. Kristoffersson, E. Carlström, Tape casting of alumina in water with an acrylic latex binder, J. Eur. Ceram. Soc. 17 (1997) 289–297.

[16] N. Joseph, J. Varghese, M. Teirikangas, T. Vahera, H. Jantunen, Ultra-low-temperature cofired ceramic substrates with low residual carbon for next-generation microwave applications, ACS Appl. Mater. Interfaces 11 (2019) 23798–23807.

[17] M. Nakahara, T. Murakami, Electronic states of Mn ions in $Ba_{0.97}Sr_{0.03}TiO_3$ single crystals, J. Appl. Phys. 45 (1974) 3795–3800.

[18] S. Thomas, M.T. Sebastian, Effect of B_2O_3-Bi_2O_3-SiO_2-ZnO glass on the sintering and microwave dielectric properties of $0.83ZnAl_2O_4$-$0.17TiO_2$, Mater. Res. Bull. 43 (2008) 843–851.

[19] O. Dernovsek, A. Naeini, G. Preu, W. Wersing, M. Eberstein, W.A. Schiller, LTCC glass-ceramic composites for microwave application, J. Eur. Ceram. Soc. 21 (2001) 1693–1697.

[20] I.J. Induja, P. Abhilash, S. Arun, K.P. Surendran, M.T. Sebastian, LTCC tapes based on Al_2O_3-BBSZ glass with improved thermal conductivity, Ceram. Int. 41 (2015) 13572–13581.

[21] M.-Y. Chen, J. Juuti, C.-S. Hsi, C.-T. Chia, H. Jantunen, Dielectric properties of ultra-low sintering temperature Al_2O_3 -BBSZ glass composite, J. Am. Ceram. Soc. 98 (2015) 1133–1136.

[22] A.G, W.J. Parker, R.J. Jenkins, C.P. Butler, Flash method of determining thermal diffusivity, heat capacity, and thermal conductivity, J. Appl. Phys. (1961) 1679–1684.

[23] Z. Lü, D. Jiang, J. Zhang, Q. Lin, Processing and properties of ZrB2-SiC composites obtained by aqueous tape casting and hot pressing, Ceram. Int. 37 (2011) 293–301.

[24] L. Wang, G. Tang, Z.K. Xu, Preparation and electrical properties of multilayer ZnO varistors with water-based tape casting, Ceram. Int. 35 (2009) 487–492.

[25] B. Bitterlich, J.G. Heinrich, Aqueous tape casting of silicon nitride, J. Eur. Ceram. Soc. 22 (2002) 2427–2434.

[26] L. Bergström, Shear thinning and shear thickening of concentrated ceramic suspensions, Colloids Surf. A Physicochem. Eng. Asp. 133 (1998) 151–155.

[27] C. Goulart, D. de Souza, Critical analysis of aqueous tape casting, sintering, and characterization of planar Yttria-Stabilized Zirconia electrolytes for SOFC, Int. J. Appl. Ceram. Technol. 14 (2017) 413–423.

[28] I.J. Induja, M.R. Varma, M.T. Sebastian, Preparation, characterization and properties of alumina-lithium aluminium borosilicate glass based LTCC tapes, J. Mater. Sci. Mater. Electron. 28 (2017) 14655–14663.

[29] O.V. Mazurin, Problems of compatibility of the values of glass transition temperatures published in the world literature, Glass Phys. Chem. 33 (2007) 22–36.

[30] J. Barta, M. Pospisil, V. Cuba, Indirect synthesis of Al_2O_3 via radiation- or photochemical formation of its hydrated precursors, Mater. Res. Bull. 49 (2014) 633–639, https://doi.org/10.1016/j.materresbull.2013.10.005.

[31] S. Lamouri, M. Hamidouche, N. Bouaouadja, H. Belhouchet, V. Garnier, G. Fantozzi, J.F. Trelkat, Control of the γ-alumina to α-alumina phase transformation for an optimized alumina densification, Bol. La Soc. Esp. Ceram. y Vidr. 56 (2017) 47–54, https://doi.org/10.1016/j.bsecv.2016.10.001.

[32] J.S. Lee, H.S. Kim, N.K. Park, T.J. Lee, M. Kang, Low temperature synthesis of α-alumina from aluminum hydroxide hydrothermally synthesized using $[Al(C_2O_4)x(OH)y]$ complexes, Chem. Eng. J. 230 (2013) 351–360, https://doi.org/10.1016/j.cej.2013.06.099.

[33] R. Faddoul, N. Reverdy-Bruas, A. Blayo, D. Chaussy, Flexography printing of silver tracks on LTCC tapes - effect of printing direction on line properties, in: Proc. - IMAPS/ACerS 8th Int. Conf. Exhib. Ceram. Interconnect Ceram. Microsystems Technol., CICMT 2012, 2012, pp. 314–321.

[34] H.I. Hsiang, C.S. Hsi, C.C. Huang, S.L. Fu, Sintering behavior and dielectric properties of $BaTiO_3$ ceramics with glass addition for internal capacitor of LTCC, J. Alloys Compd. 459 (2008) 307–310.

[35] K.T. Wang, Y. He, Z.Y. Liang, X.M. Cui, Preparation of LTCC materials with adjustable permittivity based on BaO-B_2O_3-SiO_2/$BaTiO_3$ system, Mater. Res. Bull. 65 (2015) 249–252.

[36] H. Xiang, C. Li, H. Jantunen, L. Fang, A.E. Hill, Ultralow loss $CaMgGeO_4$ microwave dielectric ceramic and its chemical compatibility with silver electrodes for low-temperature cofired ceramic applications, ACS Sustain. Chem. Eng. 6 (2018) 6458–6466.

[37] D.W. Lee, W.D. Kingery, Radiation energy transfer and thermal conductivity of ceramic oxides, J. Am. Ceram. Soc. 43 (1960) 594–607.

[38] S.B. Roshni, M.T. Sebastian, Surendran K.P, Can zinc aluminate-titania composite be an alternative for alumina as microelectronic substrate? Sci. Rep. 7 (2017) 40839.

[39] Y. Wang, G. Zhang, J. Ma, Research of LTCC/Cu, Ag multilayer substrate in microelectronic packaging, Mater. Sci. Eng. B Solid-State Mater. Adv. Technol. 94 (2002) 48–53.

[40] G. Gao, L. Hu, H. Fan, G. Wang, K. Li, S. Feng, S. Fan, H. Chen, Effect of Bi_2O_3 on physical, optical and structural properties of boron silicon bismuthate glasses, Opt. Mater. (Amst.) 32 (2009) 159–163.

[41] D.R. Lekshmi, S. Kuzhichalil Peethambharan, Ultra-low dielectric loss BiSmMoO6 flexible tapes for hybrid integrated circuits, J. Eur. Ceram. Soc. 39 (2019) 1819–1826.

[42] O.I. Pushkarev, Study of the surface strength and crack resistance of very hard ceramic materials by the microindentation method, Refract. Ind. Ceram. 43 (2002) 295–298.

[43] G. hua Chen, L. jiang Tang, J. Cheng, M. hong Jiang, Synthesis and characterization of CBS glass/ceramic composites for LTCC application, J. Alloys Compd. 478 (2009) 858–862.

[44] P. Abhilash, S.B. Roshni, P. Mohanan, K.P. Surendran, A facile development of homemade substrate using 'quench free' glass-ceramic composite and printing microstrip patch antenna on it, Mater. Des. 137 (2018) 38–46, https://doi.org/10.1016/j.matdes.2017.10.015.

[45] P. Abhilash, M.T. Sebastian, K.P. Surendran, Structural, thermal and dielectric properties of rare earth substituted eulytite for LTCC applications, J. Eur. Ceram. Soc. 36 (2016) 1939–1944.

[46] M. Maruyama, R. Matsubayashi, H. Iwakuro, S. Isoda, T. Komatsu, Silver nanosintering: a lead-free alternative to soldering, Appl. Phys. A Mater. Sci. Process. 93 (2008) 467–470.

[47] Y. Shang, C. Zhong, H. Xiong, X. Li, H. Li, X. Jian, Ultralow-permittivity glass/Al_2O_3 composite for LTCC applications, Ceram. Int. 45 (2019) 13711–13718, https://doi.org/10.1016/j.ceramint.2019.04.066.

[48] Q. Xia, C.W. Zhong, J. Luo, Low temperature sintering and characteristics of K_2O–B_2O_3–SiO_2–Al_2O_3 glass/ceramic composites for LTCC applications, J. Mater. Sci. Mater. Electron. 25 (2014) 4187–4192, https://doi.org/10.1007/s10854-014-2147-0.

[49] X. Luo, L. Ren, Y. Xia, Y. Hu, W. Gong, M. Cai, H. Zhou, Microstructure, sinterability and properties of CaO-B_2O_3-SiO_2 glass/Al_2O_3 composites for LTCC application, Ceram. Int. 43 (2017) 6791–6795, https://doi.org/10.1016/j.ceramint.2017.02.096.

[50] M. Liu, H. Zhou, X. Xu, Z. Yue, M. Leu, H. Zhu, Sintering, densification and crystallization of Ca-Al-B-Si-O glass/Al_2O_3 composites for LTCC application, J. Mater. Sci. Mater. Electron. 24 (2013) 3985–3994, https://doi.org/10.1007/s10854-013-1351-7.

[51] I.J. Induja, K.P. Surendran, M.R. Varma, M.T. Sebastian, Low κ, low loss alumina-glass composite with low CTE for LTCC microelectronic applications, Ceram. Int. 43 (2017) 736–740, https://doi.org/10.1016/j.ceramint.2016.10.002.

[52] L. Ren, X. Luo, Y. Xia, Y. Hu, H. Zhou, Fabrication of a high-performance film based borosilicate glass/Al_2O_3 ceramics for LTCC application, J. Eur. Ceram. Soc. 37 (2017) 2415–2421, https://doi.org/10.1016/j.jeurceramsoc.2017.01.031.

[53] F. Corp, Low Temperature Co-Fired Ceramic Systems A6M-E High Frequency LTCC Tape System, n.d. www.ferro.com. (Accessed November 24, 2020).

[54] GreenTape™ 951 LTCC System | Low Temperature Co-fired Ceramic, (n.d.). https://www.dupont.com/products/greentape-951-ltcc-material-system.html (Accessed November 24, 2020).

[55] Thick Film Technial Datasheets, (n.d.). https://www.heraeus.com/en/het/products_and_solutions_het/thick_film_materials/datasheets_thickfilm/datasheets_thickfilm_page.html (Accessed November 24, 2020).